Renewable Power Systems for Microgrids in Public Buildings

Miguel Quitério Simão Coelho
miguel.q.s.coelho@tecnico.ulisboa.pt

Instituto Superior Técnico, Universidade de Lisboa, Portugal
December 2021

***Abstract*— With climate change and environmental problems being one of the biggest concerns in Europe, efforts have been made to redesign the power system, enabling higher penetration of renewable energy. Energy systems, like microgrids, that allow the local integration of renewable energy generation technologies with energy storage and energy demand, will play an important role in the future power system. Due to the uncertainty in the energy generation of dispatchable generation technologies (namely photovoltaic and wind power systems), there is a need to develop modeling tools to assist energy planners in sizing and predicting the operation of energy systems like microgrids. In this work, an energy model tool capable of modeling the interaction between energy generation, using photovoltaic and wind power systems, energy storage, using lithium-ion batteries, and energy demand, has been developed in MATLAB-Simulink. The tool was developed to model the specific case of a microgrid implemented in a pilot office located in Laboratório Nacional de Energia e Geologia, and, to enhance its capabilities while evaluating and validating its performance, the developed model was compared to a commercially available software, POLYSUN, presenting a mean absolute percentage error always inferior to 5%, while guaranteeing power quality at every instant. Furthermore, the results of the tests carried out revealed the environmental and economical potential of increasing the size of the generation and storage technologies implemented in the microgrid under analysis.**

Key Words— Distributed Energy; Energy Model Tool; Energy Storage; Microgrid; Power Quality; Renewable Energy Sources.

I. INTRODUCTION

Climate change and environmental problems are one of Europe's biggest concerns. To overcome these challenges, the European Union (EU) has set ambitious environmental and energy goals, with the objective of making EU climate-neutral by 2050. Designing a low-carbon energy system by the middle of the 21st century is one of the EU's priorities, and targets have been set to drive and foster this transition [1]. The European Commission's Energy Roadmap 2050 shares the desire of developing energy systems that protect the environment, create affordable and market-orientated energy services while ensuring the security, resilience, and reliability of the energy supply. These energy systems are designed with the purpose of being integrated into infrastructures for all energy carriers, using the electrical system as support. These technologies will introduce a redesign in the power system, where most centralized individual producers will be replaced by decentralized and collective prosumers, who consume directly the energy produced.

Buildings will play an important role in this new power system, due to the diverse possibilities of on-site energy generation, and to the need of decreasing the energy consumption in this sector, which is responsible for a share of roughly 60% of the final electricity consumption in Europe [2]. The possibility of constructing and operating local small-scale power supply technologies and energy storage systems associated with energy consumption in buildings, offers environmental benefits, such as lowering the greenhouse gas emissions, by self-consuming the locally generated energy using renewable energy sources, social benefits, such as a power system more reliable, resilient, and affordable, and economical benefits because microgrids contribute to a higher energy self-sufficiency, which is also an important target of the EU, since, according to the European Commission, in 2018 EU's energy dependency rate was equal to 58% [3].

II. LITERATURE REVIEW

The concept of microgrid is used in the engineering vocabulary for more than a decade. Yet, in the existent literature, there is not a singular definition to describe it [4], since this concept covers a wide range of configurations [5]. The most used definition by researchers was proposed by the U.S. Department of Energy and states that a microgrid is ''a group of interconnected loads and distributed energy resources within clearly defined electrical boundaries that acts as a single controllable entity with respect to the grid. A microgrid can connect and disconnect from the grid to enable it to operate in both grid-connected or island mode''[6]. These energy systems are composed of distributed energy resources (DERs), loads, distribution systems, control and communication systems. DERs are composed of distributed generation technologies and energy storage systems, connected to a local distribution system [7].

In microgrids where the objective is to generate energy using

renewable energy technologies, solar photovoltaic and wind turbines are the most common distributed generation technologies implemented, since wind and solar radiation are abundant in many locations and these technologies are easy to install or integrate into a building environment. Despite these advantages, the mentioned technologies present a drawback when it comes to controlling the output power. These technologies, known as non-dispatchable, generate energy in an intermittent way, reducing the flexibility in meeting energy generation with energy demand [8]. In the literature, numerous examples of microgrids with renewable resources can be found, and an especial focus has been given to overcome the intermittence of non-dispatchable technologies in order to provide a more stable and reliable power generation, which is commonly accomplished by that integrating diverse renewable generation technologies and using energy storage systems.

Energy Storage Systems (ESSs) convert electricity into a storable energy form during high generation periods and convert the stored energy back to electricity during peak load, reducing the mismatch between the supply and demand side in microgrids and improving power quality, voltage and frequency stability, and power reliability [9]. ESSs can be divided into five groups, according to their primary source of energy, which are: electrical, mechanical, thermal, electrochemical, and magnetic [10]. Batteries due to their technological maturity and ease to design and install, when compared to other energy storage technologies, are the most used storage technology in microgrids [11].

Modeling tools play an important role in the energy system since they are a quick and cheap way to predict the performance of a system. Their role is particularly important when non-dispatchable distributed energy technologies are considered, as is the case of most microgrids, due to the variability and unpredictability of power generation, which can reflect in mismatches between demand and generation. Modeling tools can forecast these problems and present solutions to overcome them. To model a microgrid two approaches can be taken: an existing modeling tool can be used, or a tailor-made model can be developed. Tailor-made models are the most frequent method, found in the literature, to model microgrids with dispatchable energy technologies. This has to do with the higher flexibility, presented by the tailor-made models, in detailing the technical parameters of the generation technologies, and with the limitations felt by commercial tools when it comes to considering intra-hour variability and variations in the bus voltage, which is an important characteristic for networks with high PV power penetration since solar radiation can suffer high fluctuations in a short period of time [12]. From all modeling software that enable the development of tailor-made models, MATLAB-Simulink stands out as the most used tool in the literature to perform dynamic modeling and simulation of microgrids.

In 2010 [13] proposed a hybrid solar-wind system, modeled, and simulated with MATLAB-Simulink, to generate enough power to supply villages in the desert/rural areas of Iraq. In [14] the author studied the possibility of integrating energy sources, such as solar, wind, and fuel cell at the distribution level, by developing a dynamic model of a microgrid in MATLAB-Simulink, concluding that this integration produced satisfactory results, and suggesting the evaluation of a pilot scheme grid integration at a laboratory level. A renewable energy-based microgrid, composed of a solar-wind system, was proposed by [15] to supply a chosen sample number of houses at St. Martin's Island in Bangladesh, simulating the energy generation in a model developed using MATLAB-Simulink, and concluding that the microgrid could successfully supply a total of 200 houses, 20 shops and a hospital over a period of one year. In [16] the author presents a microgrid structure consisting of PV panels and a wind turbine modeled in MATLAB-Simulink and validated with real experimental data, designed to supply a household. More recently [17] modeled a building integrated hybrid microgrid, using MATLAB-Simulink, proposing an efficient power control scheme for the PV panels, wind turbine, and storage system and demonstrating an adequate output power quality with low Total Harmonic Distortion.

III. MICROGRID MATLAB-SIMULATION MODEL

The electric microgrid, intended to model in this work, is composed of five systems: four energy generation systems, constituted by two PV systems, one with 4050 W and the other with a 560 W rated power, a photovoltaic-thermal system (PVT) with an electric rated power of 690 W and a 2500 W rated power wind power system, the fifth system consists in an energy storage system, composed by a 48V Lithium-Ion battery with 660 Ah energy capacity. Since the objective of this work is to only model electric energy generation, the PVT system was approximated to an overlap between PV modules and thermal collectors, and only the PV modules were modeled. In this approximation, the effect of the thermal component of the PVT system was considered when computing the PV module's cell temperature, resulting in a lower value. These systems were modeled and tested individually and then integrated to produce the desired microgrid.

Photovoltaic System

A rooftop grid-connected photovoltaic system is normally composed of a generation unit, the PV array, and a power conditioning unit (PCU) responsible for converting the DC power generated by the PV array into usable AC power and for guaranteeing that the PV system's output voltage and frequency meet the required standard values. The PCU is

connected to a distribution board, which transfers power to the building appliances or to the grid.

The PV array was modeled using a MATLAB library block, figure 1, that implements an array of PV modules, each modeled using the 1Diode and 5 Parameters model as indicated in [18]. The user can define the number of parallel strings and the number of series-connected modules per string as well as the properties of the modules. To calculate the cell temperature, one of the inputs of the PV array block, equation 1 was used [19].

$$T_{cell} = T_{amb} + G\frac{45-20}{800} \quad (1)$$

Figure 1- PV Array block (left) and block's data (right).

A typical PCU consists of a DC-DC converter and a DC-AC Inverter. The DC-DC convert, working as a boost converter, is responsible for stepping up the slightly varying output PV array voltage to a constant higher voltage level, and for performing the maximum power point tracker (MPPT) function. The Perturb and Observe (P&O) technique was the one chosen to perform the MPPT task. This method makes incremental changes in the voltage, changing the working point in the I-V curve, and monitors the consequent changes in power, until the output voltage that produces the maximum output power is found [20]. The inverter, connected to the terminals of the boost converter, converts the DC voltage into an AC three-phase 400 V phase-to-phase voltage with a frequency of 50 Hz. The switching pattern of the invertor's transistors is determined by a controlling unit that compares the current signal at the output of the inverter with reference values. The difference between the two sets of values is used to produce transformed variables, which in turn are responsible for generating the switching pattern of the invertor's transistors. The output of the inverter is connected to the grid through an LCL filter, used to minimize the harmonic content of the output signal. The two devices were modeled based on their equivalent circuit, figure 2.

The losses of the system were calculated based on the procedure presented in [21]. It was assumed that there are three different types of losses: losses in the cables, responsible for decreasing the injected power by 4%, losses due to soiling in the PV modules, responsible for a loss equal to 2%, and losses due to degradation of the system's components, assumed to be a linear process, resulting in a continuous decrease of power equal to 0.2%/year.

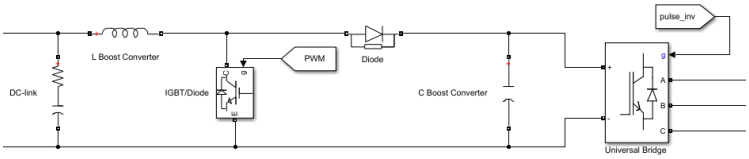

Figure 2- Power Conditioning Unit electric circuit.

Wind Power System

The wind power system is composed of a wind turbine, responsible for converting the wind kinetic energy into mechanical power, a generator, which converts the mechanical power into electricity, and a power conditioning unit, where the electrical signal produced by the generator is controlled and transformed using an AC-DC-AC converter which is connected to the grid. In the case in hands, the generator used is a Permanent Magnet Synchronous Generator (PMSG), characterized by having high efficiency and reliability.

To model the wind turbine and the generator simultaneously, the wind turbine generator power performance curve was determined from real measured data, allowing the prediction of the electric power output based solely on the wind speed. The mathematical equation that best models the power curve can be found in equation 2, where 3.5 m/s is the cut-in speed, the wind speed at which the turbine starts to generate power, the 10 m/s is the rated speed, the wind speed at which the turbine reaches rated power and 25 m/s is the cut-out speed, the wind speed at which the system shuts down for safety reasons.

$$\begin{aligned} P_e &= 0 && u < 3.5\ m/s \quad (2)\\ P_e &= 0.009u^5 - 0.5095u^4 + 8.1331u^3 - 16.209u^2 - \cdots \\ &\quad - 139.85u + 449.26 && 3.5 < u < 25\ m/s \\ P_e &= 0 && u > 25 m/s \end{aligned}$$

The PCU of a grid-connected wind power system, responsible for converting the electrical power at the output of the generator into usable power, is composed of an AC-DC-AC converter, figure 3. The rectifier, connected to the output of the generator, converts the three-phase AC signals into DC, the DC-DC boost converter receives the slightly changing voltage coming for the rectifier, and steps it up to a constant value. This converter is then connected to a DC-AC inverter, which transforms the DC voltage into an AC three-phase 400 V phase-to-phase voltage with a frequency of 50 Hz, operating in a similar way as the one described in the photovoltaic system.

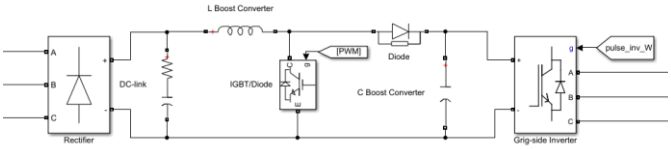

Figure 3 - Power Conditioning Unit electric circuit.

The DC-AC inverter is connected to the grid via an LCL filter, used to minimize the harmonic content of the output signals. It was assumed that the losses in the cables, are the main type of losses in this system, being responsible for decreasing the injected power by 4%.

Energy Storage System Model

The energy storage system is composed of a Lithium-Ion battery and a charging control unit. This system is responsible for storing energy when there is a surplus in energy generation and converting the stored energy back to electricity during peak load. This process is controlled by the charging control unit, which not only controls the moments at which the battery is being charged or discharged but also controls the charging and discharging rates, guaranteeing good battery usage and preservation.

To model the energy storage system, two separate blocks were developed: one for determining the status of the battery, figure 4, and one to control the charging and discharging process, figure 5. The first block calculates the battery state of charge (SOC), by calculating the difference between the power at the output of the generation units and the power required to satisfy the demand, and thus determining the available charging power or the needed discharging power of the battery. This quantity is then integrated to determine the energy stored or removed from the battery.

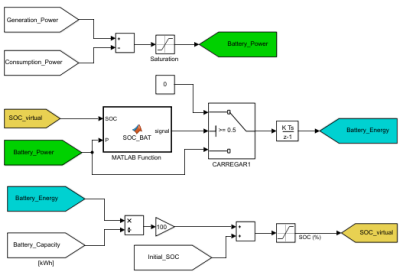

Figure 4 - Battery SOC block.

The charging control unit block is responsible for charging the battery when there is a surplus in energy generation and the battery is not fully charged yet, and for discharging the battery when the demand surpasses the generation and the minimum battery's SOC hasn't been reached (15%) while controlling the rate of charge/discharge. To do so, this block receives as inputs the battery SOC and the value of the energy balance between the energy generation systems and the energy consumption.

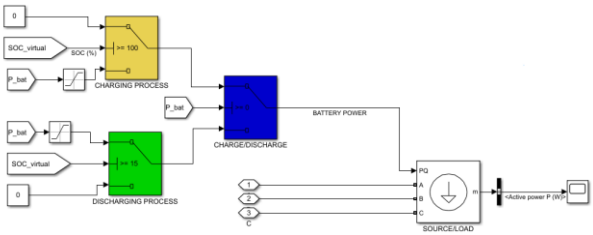

Figure 5 - Battery Control Unit.

Microgrid Model

Having modeled individually each one of the five systems, they can be integrated to produce the desired microgrid, presented in figure 6.

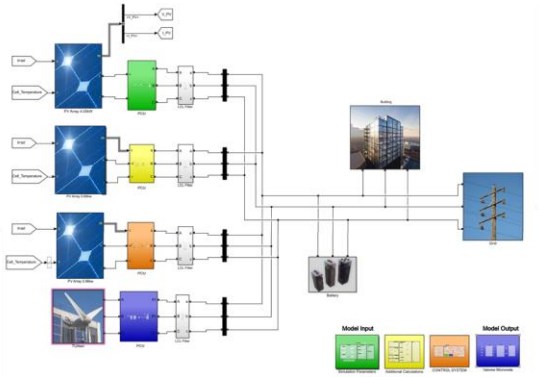

Figure 6- Microgrid MATLAB-Simulation Model.

IV. Demand Side Management

To identify the operating conditions that allow taking the most advantage of a microgrid Demand Side Management (DSM) can be used. DSM can be defined as a set of measurements, adopted by the consumption side, that modify the energy consumption pattern to promote better operation efficiency in electrical energy systems. Two of those measurements, which are of most importance in the case in hands, are load scheduling, corresponding to shifting loads from peak to off-peak hours, and optimization of battery usage, where the charge and discharge processes are controlled to allow an efficient battery usage.

Applying the two previous measurements results in an optimization problem, where the objective is to minimize the building energy costs (EC) by performing load scheduling, according to the electricity price and the renewable energy availability, and by performing intelligent battery charging/discharging control, equation 3.

$$f = Min.\ EC = \sum_{t=1}^{T} \left(P_{t\ grid} \times 1\ [hour] \times c_t\right) + CP \qquad (3)$$

In the previous equation CP is the daily contracted power cost, c_t is the electricity hourly cost for a certain hour t, and $Pt\ grid$ represents the average hourly power value that is being supplied by the grid for that same hour t, obtained from the balance between the generation power $P_{t\ generation}$, the power at the output of the energy storage system $P_{t\ battery}$, and the power demand $P_{t\ Load}$, equation 4.

$$P_{t\ grid} = P_{t\ Load} - P_{t\ generation} + P_{t\ battery} \quad (4)$$

The generation power is directly obtained from the developed program and cannot be changed, but the demand power can be optimized by optimizing the scheduling of the flexible loads, equation 5, and the power at the output of the battery can also be optimized by controlling the charging and discharging process, equation 6. In both equations $x_{t,i}$ is the hourly decision variable, indicating the state of a flexible load, in equation x, and the state of the battery, in equation x, during hour t.

$$P_{t\ Load} = P_{t\ Fixed} + P_{Flexible\ 1}\, x_{t,1} + P_{Flexible\ 2}\, x_{t,2} + \cdots + P_{Flexible\ n}\, x_{t,n} \quad (5)$$

$$P_{t\ battery} = P_{bat\_Chg} x_{t,chg} - P_{bat_{Dchg}} x_{t,dchg} \quad (6)$$

The described system is governed by some restrictions, for instance, the battery cannot be charging and discharging at the same time, this means that the summation of the two battery charging/discharging process's decision variables at a certain hour t cannot be greater than 1, the battery cannot charge to a value greater than its energy capacity and cannot discharge to a value lower than a SOC equal to 15%, and flexible loads need to meet the required daily energy consumption, meaning that they cannot consume more or less than the energy necessary to perform their daily task.

To solve the previous equation, Particle Swarm Optimization (PSO), a random search optimization technique, can be used. This technique is based on animals' behavior, especially birds and fishes that travel in groups, and use the group information to adjust their own position and velocity, reducing individuals' effort in the search for food or shelter. PSO associates each animal of the group to a single solution which could be viewed as a particle in the swarm. Particles can update their position and velocity according to the environment change, not having their movement limited by the swarm, but instead, continuously searching for the optimal solution in the possible solution space. The position vector of each particle represents a solution to the problem, which starts by being random but is continuously optimized throughout each integration, equation 7. For each iteration, the new particle n position $\vec{x}_{i+1}{}^{n}$ is based on the previous iteration position $\vec{x}_i{}^{n}$ and on the particle's velocity for that iteration $\vec{v}_{i+1}{}^{n}$. The velocity of each particle is also updated for each iteration, equation 8, being influenced by the individual particle's optimal position P_{Best}, and by the swarm's optimal position $P_{GlobalBest}$. The first refers to the position value already experienced by the particle that resulted in the best solution or that particle, and the second refers to the position experienced by any of the particles in the swarm that produced the best solution obtained for the entire swarm. To determine the other parameters the procedure described in [22] can be followed.

$$\vec{x}_{i+1}{}^{n} = \vec{x}_i{}^{n} + \vec{v}_{i+1}{}^{n} \quad (7)$$

$$\vec{v}_{i+1}{}^{n} = w_i{}^{n} \times \vec{v}_i{}^{n} + c1_i{}^{n} \times r1_i{}^{n} \times \left(P_{Best}{}^{n} - \vec{x}_i{}^{n}\right) + \cdots + c2_i{}^{n} \times r2_i{}^{n} \times \left(P_{GlobalBest} - \vec{x}_i{}^{n}\right) \quad (8)$$

To guarantee that the solutions obtained, using the procedure described, obey the problem restrictions, the penalty approach can be used [23]. This approach converts the restrictions into possible penalty values that are added to the solution of the problem obtained for each particle in each iteration, based on the number of constraints violated. Thus, if after updating its velocity and position in each iteration, the particle does not respect the restrictions, a penalty, according to the number and severity of restrictions violated, will be added to the solution increasing its value and making the solution obtained obsolete.

V. Results and Discussion

Photovoltaic System

To evaluate the performance of the PV systems, each one of the three systems was initially studied individually and then integrated to form a single model. During the study phase, where special attention was given to the performance of the MPPT technique used, the inverter controller scheme, and PCU design, each system was subjected to an irradiance profile composed of a set of constant irradiance values and a cell temperature of 25 ºC. The results obtained during these tests showed that the MPPT performed as expected, having an efficiency close to unity for all irradiance levels and that the inverter controller scheme was able to convert the DC quantities into AC three-phase, although with an efficiency 4% lower than that of a commercial inverter, but having a power coefficient close to one and respecting the acceptable power quality limits [24].

After concluding the evaluation of the performance of each PV system, the three systems were integrated to form a single model, that was validated by comparing the results obtained under real irradiance data with those obtained from an identical model developed in a commercial software, POLYSUN. To carry out the validation process, two simulations were preformed, the first consisting in a daily simulation, where a day at the beginning of January was chosen to represent the cold season, and the second in a weekly simulation, where a week in

the middle of July was chosen to represent the hot season. For these two tests, the mean absolute percentage error (MAPE) between the sets of values obtained at the output of the PV array and at the output of the inverter using the developed model and POLYSUN, was calculated. Presenting a MAPE for the daily simulation equal to 3.6% at the output of the PV array and equal to 4.2% at the output of the inverter, and a MAPE for the weekly simulation equal to 3.6% at the output of the PV array, and equal to 3.8% at the output of the inverter. In figure 7, the results obtained for the weekly simulation using the models developed in MATLAB-Simulink and POLYSUN, can be seen.

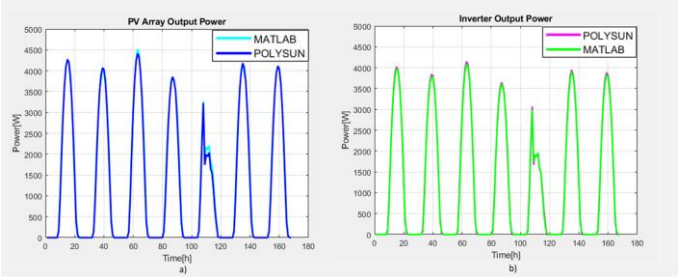

Figure 7 - Comparison between MATLAB-Simulink and POLYSUN for a weekly simulation at (a) PV Array output, (b) Inverter output

Wind Power System

To evaluate the performance of the wind power system, the developed model was submitted to a wind profile varying linearly from 0 m/s to 30 m/s, presented in figure 8. This profile was chosen because it allows to study how well the developed system models the referred power curve, which is represented in figure 6.6 b). As it can be seen, the power curve obtained at the output of the generation unit respects the values of the cut-in speed, 3.5 m/s, and of the cut-off speed, 25 m/s. In this figure, it is also possible to notice that, contrarily to what is verified in medium and large size wind turbines, the power generated by the generation unit does not remain constant after the rated wind speed is reached. This characteristic is related to the fact that for the wind turbine in hands the blade pitch control is not being applied. Furthermore, this test showed that the inverter control scheme preformed as expected, having a conversion efficiency higher than the one of the PV systems, and with an output power coefficient equal to one and respecting the acceptable power quality limits [24].

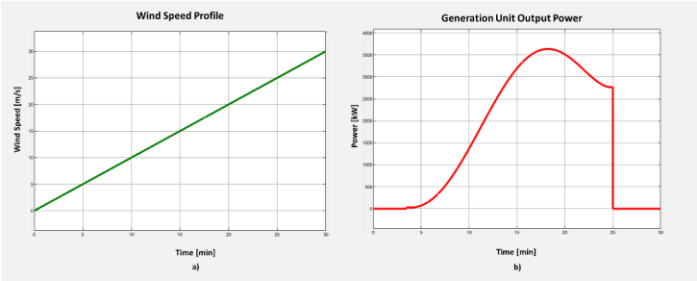

Figure 8 - Wind power system evaluation: (a) Wind speed profile, (b) Power curve at the output of the generation unit.

Energy Storage System

A similar approach to the one carried out for validating the PV system was used to validate the energy storage system. The model developed was compared to one from a commercial software, POLYSUN, and the results of the two were compared for a daily simulation and a weekly simulation. The same load profile was used for both MATLAB and POLYSUN, as well as the same battery model, which is different from the one implemented in LNEG Microgrid since POLYSUN does not have that model available in its database, and the results of the study are presented in figure 9. As it can be seen, for the two simulations, the sets of values obtained using the program developed in MATLAB-Simulink and using POLYSUN behave in a similar way, indicating that the amount of energy that is being stored in both cases is equal and that the charging and discharging processes occurs at the same instant and at the same rate in both cases. The MAPE between the two sets of values is equal to 1% for the daily simulation and 1.2% for the weekly simulation.

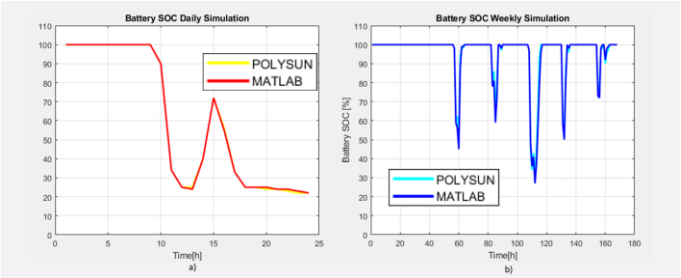

Figure 9 - Comparison between MATLAB-Simulink and POLYSUN battery SOC for (a) a daily simulation, (b) a weekly simulation.

Demand Side Management

With the objective of evaluating the performance of the developed demand-side management program, a day ahead study of the daily energy bill for three different days was performed. To carry out this study, it was considered that the consumption was composed of two types of loads, fixed and flexible, and the fixed loads' consumption pattern was extracted

from an office consumption profile, present in POLYSUN data-based, while three loads of 1 kW nominal power were considered as the controllable loads, each consuming a total of 3 kWh/day. It was also considered that the consumer had an energy supply tariff scheme characterized by three different periods: peak, intermediate, and off-peak, whose price values were obtained by consulting the website of the Portuguese retailer NOSSA Energia [25].

In table 1 the results of the test carried out can be found. As it can be seen, the optimization process is able to lower the daily energy bill for each one of the optimization techniques used, having a maximum standard deviation between runs, for each case, of 11 cents. Performing simultaneously battery control and load scheduling stands out as the best option to further decrease the daily costs, for the three days considered. Only performing battery control produces better results than only performing load scheduling, but this fact does not necessarily apply to every situation. If the number of loads or the nominal power of each current load was increased, the importance of load scheduling in the total process would also increase, and performing load scheduling would produce better results than only performing battery control. By performing this test, it is possible to conclude that associating DSM to the microgrid can really help in defining the operating conditions that allow the microgrid to be used in the most efficient way.

	Battery Control			Load Scheduling			Battery Control + Load Scheduling		
	JAN	JUL	SET	JAN	JUL	SET	JAN	JUL	SET
Number of Runs	10	10	10	10	10	10	10	10	10
Original Price Value [€/day]	3.14	2.30	2.16	3.14	2.30	2.16	3.14	2.30	2.16
Optimization Average Price Value [€/day]	2.68	2.00	1.69	2.88	2.06	2.08	2.58	1.39	1.50
Standard Deviation	0.03	0.06	0.03	0.10	0.11	0.11	0.10	0.10	0.11

Table 1 - Results of the optimization process.

Microgrid

After individually validating each system's model, they were integrated to form the desired microgrid model. With the objective of studying the behavior of the microgrid implemented in LNEG's pilot office building, a yearly simulation was carried out. The weather data used to perform this test was obtained using Meteonorm, being Lisbon the chosen location for the system, and the consumption data was provided by LNEG, being this data a realistic approximation of the pilot real consumption.

First, the amount of energy generated by each type of technology was studied, represented in figure 10. As it can be seen, the energy generated by the three PV systems is much bigger than the one generated by the wind power system, between three to four times more in the cold season months (November to February) and between four to six times more in the hot season months (March to October). This mismatch between generation units is not only due to the difference in the installed rated power, 5.3 kW for the PV systems and 2.5 kW for the wind power system but mainly because the windspeed hardly ever reaches the wind power system rated speed (10 m/s), meaning that this system is always producing energy below its capacity. This shows that, although wind power systems have the ability to generate energy during the entire day, combining PV systems with energy storage systems, like batteries, presents to be a more effective way of meeting the consumption needs, at least for a building located in Lisbon.

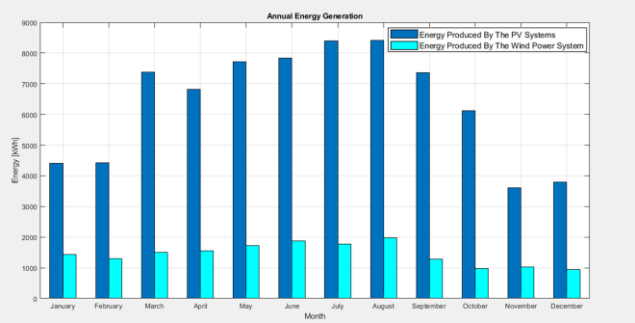

Figure 10 - Microgrid annual energy generation.

Having studied the yearly generation pattern, the analysis was expanded to include the energy storage system and the consumption needs, enabling the study of the microgrid as a whole. The results of the microgrid annual behavior are represented in figure 11, on a monthly basis. As it can be seen, the consumption surpasses the energy generation every month. In fact, the energy generated during a year by the microgrid (9063 kWh) only accounts for 28% of the total energy consumed in the building (32228.3 kWh), the missing 72% are extracted from the grid (23165.3 kWh). Since the objective of implementing a microgrid is to increase the energy independence of the building while increasing the share of renewable energy consumed, it is possible to conclude that there is room for improvement when it comes to the configuration design of this microgrid.

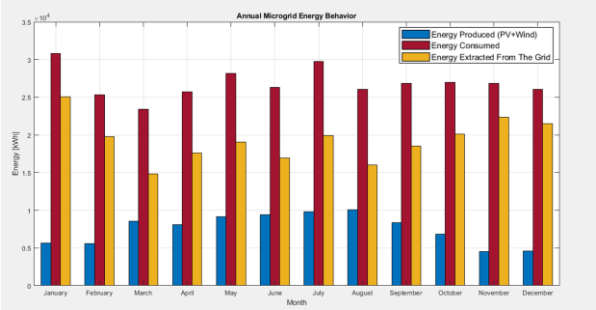

Figure 11 - Microgrid annual energy generation, energy consumption, and energy extracted from the grid.

With the objective of reducing the energy extracted from the grid while maintaining the consumption pattern, the installed nominal generation power was increased. Since the PV systems were the ones with a higher utilization factor, it would be more productive to maintain the wind generation system nominal power as it is and increase the PV systems nominal power. Figure 12 represents the variation in energy generation and energy extracted from the grid when the PV systems installed power is increased. As it can be seen, by increasing the installed power, the energy generation, represented in blue, increases in a linear way, and the energy extracted from the grid, represented in yellow, decreases towards a horizontal asymptote. It can be seen that for an installed power of 4.2 times the real system PV rated power and for an installed power of 4.6 times the real system PV rated power, the energy extracted from the grid remains almost the same, indicating that there is no more advantage in keeping increasing the PV system installed power, meaning that the limit in the total amount of power that can be installed was reached.

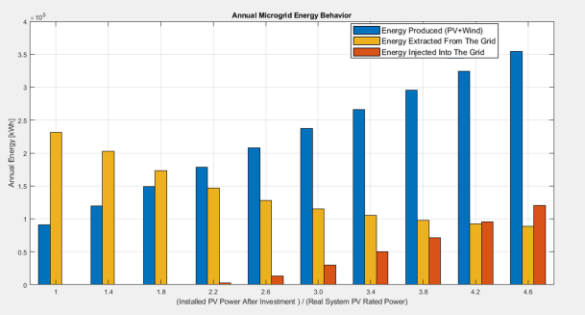

Figure 12 - Microgrid energy generation and energy extracted from the grid for different installed PV rated power.

To further decrease the amount of energy extracted from the grid, the battery energy capacity was increased, which allows storing more energy in periods where the energy generation surpasses the energy demand, decreasing the energy injected into the grid, and supplying more energy in periods where the energy demand surpasses the generation, decreasing the energy extracted from the grid. In figure 13 the evolution of the energy extracted from the grid with the increase of the energy capacity for different configurations of the PV system rated power can be seen. This study shows the improvement possibilities of rethinking the design of the microgrid under analysis, taking as an example, the option of increasing the PV system nominal power to a value 4.6 times bigger (24.38 kW) than the rated power of the system implemented in the pilot (5.30 kW) and increasing the battery capacity 1.8 times (57 024Wh) than the current battery energy capacity (31 680Wh) the percentage of energy generated by the microgrid generation units would account for 86% of the total energy consumption, instead of the initial 28%, and the energy extracted from the grid would decrease from 23165.3 kWh to 4669.5 kWh.

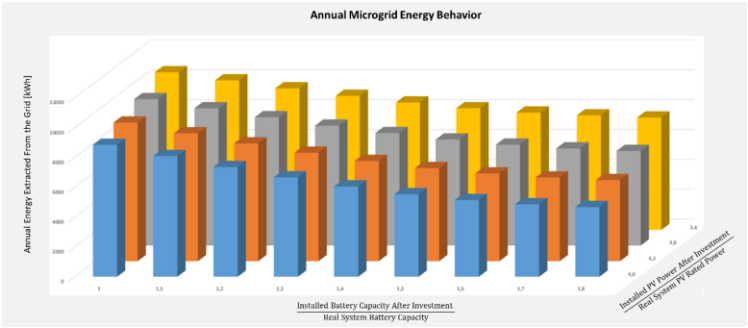

Figure 13 - Microgrid energy extracted from the grid for different battery energy capacities.

As a final remark, the economical benefits of performing a redesign in the microgrid configuration were evaluated by calculating the simple payback period and the Net Present Value (NPV) of the investment, equations 9 and 10 respectively. To do so, two parameters were computed: the investment cost, which is the upfront cost related to installing the necessary equipment and the cost associated with maintenance and equipment replacement throughout the service life of the system, and the value of the annual savings, resulting from the decrease in the energy extracted from the grid. The value of the investment was determined by defining the unitary cost of each technology and multiplying these values by the desired modifications in the microgrid configuration. The value of the annual savings was determined by computing the difference between the annual current energy bill and the annual energy bill if the investment was carried out.

$$Payback = \frac{Investment}{Annual\ Savings} \tag{9}$$

$$NPV = -I_{nv_0} + \sum_{j=1}^{T} \frac{Cf_j}{(1+i)^j} \tag{10}$$

In table 2, the payback period for the different installation conditions can be found. This quantity ranges from a value equal to 5.16 years, for an installed power equal to 1.4 times the real PV system rated power, to a value equal to 10.58 years, corresponding to an increase of 4.6 times the PV installed power and 1.8 times the battery energy capacity. It is possible to see that, although increasing the battery capacity increases the microgrid annual savings, the payback period for each fixed installed PV power does not decrease if the battery installed capacity is bigger than the one currently installed in LNEG's microgrid, showing that betting in PV systems is the most economical advantage option in the case under analysis. It is also important to notice that, to calculate the payback period, the expected life of each equipment was determined in order to

correctly estimate the investment cost. Since the expected service life of a PV module (20 years) and an inverter (up to 15 years) are bigger than the maximum payback period, there were not any additional costs concerning the PV system than the initial investment. In the case of the battery cell, according to the information presented in [26], it has an expected service life of 6.30 years, meaning that, for installations with a payback period superior to the battery service life, the costs of buying a second unit were considered as an investment.

	Investment Payback Period [years]								
	Installed Battery Capacity After Investment to Real System Battery Capacity								
Installed PV Power After Investment to Real PV System Rated Power	1.0	1.1	1.2	1.3	1.4	1.5	1.6	1.7	1.8
1.4	5.16	-	-	-	-	-	-	-	-
1.8	5.17	-	-	-	-	-	-	-	-
2.2	5.34	-	-	-	-	-	-	-	-
2.6	5.82	6.96	6.84	7.37	7.93	8.52	9.12	9.73	10.35
3.0	6.49	7.40	6.47	7.54	7.92	8.31	8.74	9.20	9.68
3.4	7.19	7.98	7.71	7.97	8.23	8.52	8.85	9.22	9.61
3.8	7.91	8.59	8.28	8.46	8.67	8.90	9.17	9.48	9.83
4.2	8.70	9.25	8.88	9.00	9.16	9.34	9.57	9.85	10.18
4.6	9.48	9.95	9.54	9.59	9.68	9.82	10.02	10.27	10.58

Table 2 - Investment Payback Period after considering the service life of the equipment.

To complement the economic analysis, the NPV of each one of the investments options was computed using equation 10, where I_{nv_0} represents the initial investment, Cf_j the savings in year j, T the period under analysis and i the discount rate. The NPV was calculated for a period of 15 years, the lifetime of the PV system, and with a discount rate equal to 0.95, representing a risk-free rate [27]. It was assumed that the battery cells were replaced after 5 years of utilization, meaning that for the cash flows of years 5 and 10 the cost of replacing the battery was subtracted from the yearly energy savings. The results of the analysis are presented in table 3, the NPV ranges from 2.29k€ to 12.60k€, for an installation power 3 times bigger than the real PV system rated power, and it is possible to see that increasing the battery capacity has no economic advantage. The evaluation of the NVP together with the assessment of the payback period shows that redesigning the microgrid configuration not only increases the environmental benefits of the microgrid because the share of renewable energy generated would increase, but also presents a good investment possibility.

	Net Present Value [k€]								
	Installed Battery Capacity After Investment to Real System Battery Capacity								
Installed PV Power After Investment to Real PV System Rated Power	1.0	1.1	1.2	1.3	1.4	1.5	1.6	1.7	1.8
1.4	3.75	-	-	-	-	-	-	-	-
1.8	7.46	-	-	-	-	-	-	-	-
2.2	10.63	-	-	-	-	-	-	-	-
2.6	12.27	10.00	10.45	9.33	8.07	6.70	5.25	3.78	2.29
3.0	12.60	10.64	11.36	10.67	9.77	8.77	7.60	6.28	4.89
3.4	12.39	10.51	11.45	10.91	10.26	9.49	8.51	7.34	6.07
3.8	11.72	9.98	11.06	10.64	10.10	9.42	8.55	7.50	6.28
4.2	10.58	9.06	10.30	10.00	9.56	8.97	8.15	7.13	5.92
4.6	9.28	7.83	9.18	9.02	8.71	8.20	7.39	6.45	5.26

Table 3 - Net Present Value of the different investments.

VI. CONCLUSIONS

The proposed work focused on developing an energy model tool capable of modeling the interaction between energy demand and energy generation in public buildings, with a special focus on studying a microgrid implemented on a pilot office owned and managed by LNEG. To accomplish this objective, a microgrid model was developed using MATLAB-Simulink, presenting good results under different operating conditions and when compared to commercially available software, such as POLYSUN. During the development of this work, a conclusion was reached that to fully take advantage of the microgrid capabilities, a microgrid general controller based on demand-side management (DSM) could be developed. So, although this was not the core of the present work, a DSM program capable of performing load scheduling and battery control was developed in MATLAB, using particle swarm optimization. After evaluating and validating the model, a yearly simulation, to study the behavior of the microgrid throughout one year, was carried out. With this simulation, it was possible to conclude that, for the consumption needs of the pilot, the microgrid energy generation only accounts for a small fraction of the total energy consumed in the building, indicating that there is an investment potential in increasing the currently installed generation rated power. As a final remark, it is important to notice that, although the presented program was developed to model a specific microgrid, the developed tool is modular, scalable, and easily adapted to other microgrid configurations, including different number and types of energy generation systems.

REFERENCES

[1] "2030 climate & energy framework | Climate Action.", European Commission, https://ec.europa.eu/clima/policies/strategies/2030_en#tab-0-0 (accessed Feb. 15, 2021).

[2] Agora Energiewende, "European Energy Transition 2030: The Big Picture," pp. 11–21, 2019, [Online]. Available: https://www.agora-energiewende.de/fileadmin2/Projekte/2019/EU_Big_Picture/153_EU-Big-Pic_WEB.pdf.

[3] "From where do we import energy and how dependent are we?", European Commission, https://ec.europa.eu/eurostat/cache/infographs/energy/bloc-2c.html (accessed Feb. 15, 2021).

[4] D. E. Olivares *et al.*, "Trends in microgrid control," *IEEE Trans. Smart Grid*, vol. 5, no. 4, pp. 1905–1919, 2014, doi: 10.1109/TSG.2013.2295514.

[5] "So, What is a Microgrid, Exactly? : HOMER Microgrid News.", HOMER Energy, https://microgridnews.com/what-is-a-microgrid/ (accessed Feb. 19, 2021).

[6] D. T. T. and M. A. S. I., "US Energy defenition Microgrid," 2012, [Online]. Available: http://dx.doi.org/10.1016/j.tej.2012.09.013.

[7] S. Parhizi, H. Lotfi, A. Khodaei, and S. Bahramirad, "State of the art in research on microgrids: A review," *IEEE Access*, vol. 3, no. July, pp. 890–925, 2015, doi: 10.1109/ACCESS.2015.2443119.

[8] N. M. Kumar *et al.*, "Distributed Energy Resources and the Application of AI, IoT, and Blockchain in Smart Grids," *Energies*, vol. 13, no. 21, p. 5739, 2020, doi: 10.3390/en13215739.

[9] H. Nazaripouya, Y.-W. Chung, and A. Akhil, "Energy Storage in Microgrids: Challenges, Applications and Research Need," *Int. J. Energy Smart Grid*, vol. 3, no. 2, pp. 60–70, 2019, doi: 10.23884/ijesg.2018.3.2.02.

[10] A. A. Khodadoost Arani, G. B. Gharehpetian, and M. Abedi, "Energy Storage 1," *Int. J. Electr. Power Energy Syst.*, vol. 107, no. December 2018, pp. 745–757, 2019, doi: 10.1016/j.ijepes.2018.12.040.

[11] D. Akinyele, J. Belikov, and Y. Levron, "Battery Storage Technologies for Electrical Applications: Impact in Stand-Alone Photovoltaic Systems," *Energies*, vol. 10, no. 11, pp. 1–39, 2017, doi: 10.3390/en10111760.

[12] J. Huang and R. J. Davy, "Predicting intra-hour variability of solar irradiance using hourly local weather forecasts," *Sol. Energy*, vol. 139, pp. 633–639, 2016, doi: 10.1016/j.solener.2016.10.036.

[13] S. S. Dihrab and K. Sopian, "Electricity generation of hybrid PV/wind systems in Iraq," *Renew. Energy*, vol. 35, no. 6, pp. 1303–1307, 2010, doi: 10.1016/j.renene.2009.12.010.

[14] V. S. Bugade and P. K. Katti, "Dynamic modelling of microgrid with distributed generation for grid integration," *Int. Conf. Energy Syst. Appl. ICESA 2015*, no. Icesa, pp. 103–107, 2016, doi: 10.1109/ICESA.2015.7503321.

[15] A. Muhtadi, "Solar PV & DFIG based Wind Energy Conversion System for St . Martin ' s Island," *2017 IEEE 3rd Int. Conf. Eng. Technol. Soc. Sci.*, 2017, doi: 10.1109/ICETSS.2017.8324152.

[16] M. Puianu, R. O. Flangea, N. Arghira, and S. S. Iliescu, "Microgrid simulation for smart city," *Proc. 2017 IEEE 9th Int. Conf. Intell. Data Acquis. Adv. Comput. Syst. Technol. Appl. IDAACS 2017*, vol. 2, pp. 607–611, 2017, doi: 10.1109/IDAACS.2017.8095164.

[17] A. Shaqour, H. Farzaneh, Y. Yoshida, and T. Hinokuma, "Power control and simulation of a building integrated stand-alone hybrid PV-wind-battery system in Kasuga City, Japan," *Energy Reports*, vol. 6, pp. 1528–1544, 2020, doi: 10.1016/j.egyr.2020.06.003.

[18] S. Shongwe and M. Hanif, "Comparative Analysis of Different Single-Diode PV Modeling Methods," *IEEE J. Photovoltaics*, vol. 5, no. 3, pp. 938–946, 2015, doi: 10.1109/JPHOTOV.2015.2395137.

[19] R. Castro, "Renewable Energy Sources and Dispersed Power Generation, Support text for Renewable Energy Course, IST," no. September. 2018, [Online]. Available: https://fenix.tecnico.ulisboa.pt/disciplinas/ERPD36451113264/2019-2020/2-semestre.

[20] R. Bhukya, "Performance investigation on novel MPPT controller in solar photovoltaic system," doi: 10.1016/j.matpr.2021.07.286.

[21] "2019 Vela Solaris AG.", V. S. AG, https://www.velasolaris.com/ (accessed Mar. 03, 2021).

[22] R. Faia, T. Pinto, Z. Vale, and J. M. Corchado, "Strategic Particle Swarm Inertia Selection for Electricity Markets Participation Portfolio Optimization," *Appl. Artif. Intell.*, vol. 32, no. 7–8, pp. 745–767, 2018, doi: 10.1080/08839514.2018.1506971.

[23] A. R. Jordehi, "A review on constraint handling strategies in particle swarm optimisation," *Neural Comput. Appl.*, vol. 26, no. 6, pp. 1265–1275, 2015, doi: 10.1007/s00521-014-1808-5.

[24] IEEE Std 519, "IEEE Std 519-2014 (Revision of IEEE Std 519-1992), IEEE Recommended Practice and Requirements for Harmonic Control in Electric Power Systems," *IEEE Std 519-2014 (Revision IEEE Std 519-1992)*, vol. 2014, pp. 1–29, 2014, [Online]. Available: http://ieeexplore.ieee.org/servlet/opac?punumber=6826457.

[25] "NOSSA Energia - Homepage.", NOSSA Energia, https://nossaenergia.pt/ (accessed Aug. 11, 2021).

[26] "Sunlight RES OPzS 660Ah 12/24/48v batteries.", SOLARSHOP, https://www.solarshop.pt/index.php?route=product/product&product_id=88 (accessed Jul. 13, 2021).

[27] "Taxa de Juro.", Banco Portugal, https://www.bportugal.pt/sites/default/files/anexos/10-taxas_juro_bancarias.pdf (accessed Jul. 16, 2021).